

ISTITUTO NAZIONALE DI FISICA NUCLEARE

Sezione di Milano

INFN/BE-92/02

18 Giugno 1992

P. Vergani, E. Gadioli, E. Vaciago, P. Guazzoni, L. Zetta, G. Ciavola, M. Jaskola,
P.L. Dellerà, V. Campagna, C. Marchetta:

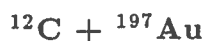
**STUDY OF ^{12}C AND ^{16}O INTERACTIONS WITH NUCLEI AT
INCIDENT ENERGIES VARYING FROM 5 TO 10 MeV/AMU**

I - $^{12}\text{C} + ^{197}\text{Au}$

INFN/BE-92/02
18 Giugno 1992

STUDY OF ^{12}C AND ^{16}O INTERACTIONS WITH NUCLEI
AT INCIDENT ENERGIES VARYING FROM 5 TO 10 MeV/AMU

I



P. Vergani^{b)}, E. Gadioli^{a,b)}, E. Vaciago^{a,b)}, P. Guazzoni^{a,b)}, L. Zetta^{a,b)}
G. Ciavola^{c)}, M. Jaskola^{d)}, P. L. Delleri^{b)}, V. Campagna^{c)}, C. Marchetta^{c)}

^{a)} *Dipartimento di Fisica, Università di Milano*

^{b)} *Istituto Nazionale di Fisica Nucleare, Sezione di Milano*

^{c)} *Laboratorio Nazionale del Sud, Catania*

^{d)} *Soltan Institute for Nuclear Studies, Warsaw*

ABSTRACT

The experimental excitation functions for production of $^{206,205,204,203}\text{At}$, $^{205,204,203}\text{g}$, ^{202}Po , $^{203,202,201}\text{g}$, ^{200}g , $^{199}\text{g}\text{Bi}$, ^{201}g , $^{200,199}\text{g}\text{Pb}$, $^{199,198}\text{m}$, $^{198}\text{g}\text{Tl}$ in the reaction $^{12}\text{C} + ^{197}\text{Au}$ at incident energies between 57 and 97 MeV have been measured by activation techniques at the Laboratorio Nazionale del Sud. These data, together with those of other authors, allow one to deduce the cross-section for (i) complete fusion of C with Au followed by decay through particle evaporation, and (ii) incomplete fusion of, respectively, a ^8Be and an α particle, from C break-up, with Au. Summing these cross-sections with the experimental fission cross-section one obtains the reaction cross-section for interaction of C with Au between 57 MeV and 120 MeV.

1. Introduction.

This Report is the first of a series scheduled to report the results of the measurements of (i) excitation functions for production of heavy residues and (ii) recoil range distributions of heavy residues in reactions induced by ^{12}C and ^{16}O ions on medium-heavy and heavy nuclei at energies varying from the Coulomb barrier up to the maximum energy available with the MP Tandem accelerator of the Laboratorio Nazionale del Sud (LNS) in Catania.

This systematic investigation was suggested by the consideration of the conclusions reached in the analysis of the heavy residue recoil range distributions in the reaction $^{12}\text{C} + ^{197}\text{Au}$ at an incident energy of 120 MeV^{1,2} and of a preliminary study of the excitation functions for production of At, Bi and Tl isotopes in the same reaction at incident energies varying from about 60 to about 120 MeV,³⁻⁵ which indicate that these experimental data provide invaluable information on both the incomplete fusion of these ions and the emission of pre-equilibrium nucleons in the course of the de-excitation cascade of the composite nucleus created in the projectile-target interaction. Even at the low incident energies considered the cross-sections for both these processes are far from being negligible.

In this report we present the results of the measurement of the excitation functions for production of At, Po, Bi, Pb and Tl isotopes in the $^{12}\text{C} + ^{197}\text{Au}$ reaction at incident energies varying from 57 to 97 MeV. As mentioned above, experimental excitation functions for production of At, Bi, Tl isotopes were already reported in literature³⁻⁶. However, as discussed later, there is a serious disagreement between some of these data.^{3,4,6}

Section 2 of this Report describes the experimental set up and the experimental results, and Section 3, the comparison with previous experimental information. In Section 4 the reaction cross-sections and the cross-sections for complete and incomplete fusion, that one deduces from these data, are discussed.

2. Experimental results.

The cross-sections for production of $^{206,205,204,203}\text{At}$, $^{205,204,203g,202}\text{Po}$, $^{203,202,201g,200g,199g}\text{Bi}$, $^{201g,200,199g}\text{Pb}$, $^{199,198m,198g}\text{Tl}$ in the reaction $^{12}\text{C} + ^{197}\text{Au}$ have been measured at nine energies between 57 and 97 MeV, in 5 MeV steps.

Au targets with thickness of about $800 \mu\text{g}/\text{cm}^2$ and Al catchers of $810 \mu\text{g}/\text{cm}^2$ thickness, downstream each target, were irradiated in a dedicated chamber⁷ on the 40° channel of the LNS MP Tandem.

Up to 77 MeV we used a 5^+ C beam with average beam intensities up to 600 e-nA (in evaluating the beam intensity we took into account that passing through the target and the catcher the C beam was completely stripped), at higher energies a 6^+ C beam with intensities up to about 300 e-nA. The beam spot had a diameter smaller than about 4 mm.

The irradiation times varied between 30 and 60 minutes according to the half-lives of the isotopes that were expected to be produced with the highest intensity at the various energies. Since the irradiation times were comparable or even longer than the half-lives of several of the isotopes produced, the fluence of the carbon beam was monitored *via* computer every 30 s to allow one to take into account the fluctuations in beam intensities when evaluating the production cross-sections.

After irradiation, the γ ray activities induced both in the Au target and the Al catcher were counted for several days with four 25-30% efficiency Ge(Hp) counters.

The γ -ray spectra thus obtained have been analysed with the codes GAMANAL⁸ and DECAY⁹ using for the γ -lines, identifying the various isotopes produced, the half-lives, energies and abundances given by Reus *et al.*¹⁰ and listed in Table I. However, in the case of ^{205}At we used for the abundance of the 719.3 keV γ -line the value 0.422 given in Refs. [11-13] instead of the value 0.27 as suggested by Reus *et al.*¹⁰ This choice is motivated by the fact that with this value of the abundance the absolute cross-sections for production of ^{205}At , measured in this experiment, are in excellent agreement with the cross-sections measured by Bimbot *et al.*⁴ by detecting

Table I

Half-lives, energies and abundances of characteristic γ -lines for the radioactive residues analysed. The values given for these quantities are from Reus *et al.* ¹⁰ except the abundance of the 719.3 keV line of ²⁰⁵At taken from Refs. [11-13].

Residue	$T_{1/2}$ (Hours)	E γ (keV)	Abundance %
²⁰⁶ At	0.49	396	48.3
		477.1	86.7
		700.7	98.
²⁰⁵ At	0.437	719.3	42.2
²⁰⁴ At	0.153	425	66
		515.2	90
		608	20
		683.3	94
²⁰⁵ Po	1.8	836.8	19.2
		849.8	25.5
		872.4	36.9
²⁰⁴ Po	3.53	884.0	30.3
		1016.3	24.4
		1040.0	9.73
²⁰³ Po ^y	0.612	214.8	14.6
		893.5	19
		908.6	56
		1090.9	19.6
²⁰² Po	0.745	165.7	8.55
		688.6	50
²⁰³ Bi	11.76	896.9	13.1
		1034.0	8.84
²⁰² Bi	1.72	422.1	83.7
		657.5	60.6
		960.7	99.3
²⁰¹ Bi ^y	1.80	786.4	9.66
		936.2	11.5
²⁰⁰ Bi ^y	0.61	462.3	98
		1026.5	100
¹⁹⁹ Bi ^y	0.45	842	15.7
		946	15.4
		1053	10.5
²⁰¹ Pb ^y	9.33	361.2	9.69
		946.0	7.34
²⁰⁰ Pb	21.5	147.6	37.7
		257.2	4.5
¹⁹⁹ Pb ^y	1.5	353.4	13.9
		366.9	64.8
¹⁹⁹ Tl	7.42	208.2	12.2
		247.3	9.2
		455.5	12.3
¹⁹⁸ Tl ^m	1.87	282.8	28
		587.2	51
¹⁹⁸ Tl ^y	5.3	411.8	81.8

the induced α activity.

Most of the isotopes are produced either directly in the $^{12}\text{C} + ^{197}\text{Au}$ interaction (independent yield, I), and through decay of higher Z precursors with considerably smaller half-lives (cumulative yield, C). Due to the short half-lives of many of the precursors, for most of the isotopes produced we have only obtained the cumulative yield by analysing the induced activities, at times considerably longer than the precursor half-lives, by a simple exponential (one component) decay curve. It may be shown (see the Appendix) that the cumulative cross-sections are given for each isotope by a sum of the cross-section for independent production and the cross-sections for production of the precursors multiplied by numerical coefficients whose value depends on the branching ratios for the decay of the precursor to the isotope considered and the half-life of the precursor and the isotope.

The expressions of these cumulative cross-sections are given in Table II. In evaluating the coefficients multiplying the precursor cross-sections contributing to each cumulative cross-section we have used the half-lives and decay branching ratios given by Reus *et al.*¹⁰

It is difficult to give a very precise estimate of the error affecting each of the cross-section given in the following since, in addition to the sources of error considered later, this error depends on the possible presence of γ -lines of energy and half-life comparable to those of the characteristic gamma lines (CGL). To reduce the error due to this cause we analysed up to four CGL for each isotope. The cross-section for production of the isotope was then obtained as a weighted mean of the values deduced from the activity of each CGL. As a general rule, the decay curves corresponding to the different γ -lines were of comparable quality, thus we used as weight factor the inverse of the variance corresponding to each cross-section, evaluated by DECAY code considering the statistical uncertainty of the measured activities at the different times and the scattering of the measured activities around the best fit decay curve, instead of the abundance of the CGL lines, as frequently done.

Even considering several CGL for each isotope, the values of the cross-sections which are given in Tables III to VII are affected by an uncertainty of the order of

Table II

Cross-sections for independent production and precursor contributions to the production of the measured nuclides.

<i>Residue</i>	<i>Contribution to Cumulative Nuclide Production</i>
^{205}Po	$^{205}\text{Po} + 1.19^{205}\text{At}$
^{204}Po	$^{204}\text{Po} + ^{204}\text{At}$
$^{203}\text{Po}^y$	$^{203}\text{Po}^y + 0.99^{203}\text{Po}^m + 0.86^{203}\text{At}$
^{203}Bi	$^{203}\text{Bi} + 1.05^{203}\text{Po}^y + 1.05^{203}\text{Po}^m + 0.74^{203}\text{At} + 0.12^{207}\text{At}$
^{202}Po	$^{202}\text{Po} + 0.94^{202}\text{At}$
^{202}Bi	$^{202}\text{Bi} + 1.75^{202}\text{Po} + 1.58^{202}\text{At}$
$^{201}\text{Bi}^y$	$^{201}\text{Bi}^y + 0.19^{201}\text{Bi}^m + 1.15^{201}\text{Po}^y + 1.12^{201}\text{Po}^m + 0.34^{201}\text{At} + 0.13^{205}\text{At}$
$^{201}\text{Pb}^y$	$^{201}\text{Pb}^y + 1.12^{201}\text{Bi}^m +$ $+ 1.24^{201}\text{Bi}^y + 1.25^{201}\text{Po}^y + 1.23^{201}\text{Po}^m + 0.36^{201}\text{At} + 0.13^{205}\text{At}$
$^{200}\text{Bi}^m$	$^{200}\text{Bi}^m + 1.34^{200}\text{Po} + 0.89^{200}\text{At}$
$^{200}\text{Bi}^y$	$^{200}\text{Bi}^y + 0.06^{204}\text{At}$
^{200}Pb	$^{200}\text{Pb} + 1.03^{200}\text{Bi}^y + 1.03^{200}\text{Bi}^m + 0.88^{200}\text{Po} + 0.57^{200}\text{At} + 0.05^{204}\text{At}$
$^{199}\text{Bi}^y$	$^{199}\text{Bi}^y + 1.09^{199}\text{Po}^y + 0.75^{199}\text{Po}^m + 0.43^{203}\text{At}$
$^{199}\text{Pb}^y$	$^{199}\text{Pb}^y + 1.04^{199}\text{Pb}^m +$ $+ 1.45^{199}\text{Bi}^y + 1.78^{199}\text{Bi}^m + 1.35^{199}\text{Po}^y + 0.95^{199}\text{Po}^m + 0.49^{203}\text{At}$
^{199}Tl	$^{199}\text{Tl} + 1.25^{199}\text{Pb}^y + 1.26^{199}\text{Pb}^m +$ $+ 1.33^{199}\text{Bi}^y + 1.32^{199}\text{Bi}^m + 0.85^{199}\text{Po}^m + 1.19^{199}\text{Po}^y + 0.42^{203}\text{At}$
$^{198}\text{Tl}^m$	independent yield
$^{198}\text{Tl}^y$	$^{198}\text{Tl}^y + 0.73^{198}\text{Tl}^m + 1.83^{198}\text{Pb} + 1.90^{198}\text{Bi}^y + 0.57^{198}\text{Po} +$ $+ 0.04^{202}\text{Po} + 0.27^{202}\text{At}$

15 % due mainly to (i) the uncertainty in the measurement of target thickness and local thickness disuniformities (≈ 5 %), (ii) the uncertainty in the measurement of the beam fluence (≤ 5 %), (iii) the uncertainty in the abundance of CGL (up to 10 %), (iv) statistical errors in γ intensity, background subtraction, detector dead time (a few percent all together).

A few comments concerning each single determination may be useful (for each isotope the CGL energies and abundances are those given in Table I).

^{206}At and ^{204}At (independent production, I)

The cross-sections for production of these isotopes are the weighted mean of the values obtained through the analysis of, respectively, three and four γ -lines.

^{205}At (I)

The cross-section for production of this isotope has been obtained from the analysis of the more intense characteristic γ -line. The use for this line of the abundance 0.27 given by Reus *et al*¹⁰ leads to cross-sections systematically higher than those given by Bimbot *et al*⁴. On the other hand, excellent agreement with these experimental data, obtained by measuring the induced α -particle radioactivity, was found using the abundance 0.422 suggested in Refs. [11-13].

^{203}At (I)

The cross-section for production of this isotope was obtained from the cumulative cross-section for production of $^{199}\text{Bi}^g$, in the hypothesis (see Table II) of a negligible independent production of $^{199}\text{Bi}^g$ and ^{199}Po in the energy range considered.

The measured cross-sections for production of these isotopes are given in Table III and shown by solid dots in Fig. 1.

^{205}Po , ^{204}Po , $^{203}\text{Po}^g$ and ^{202}Po (cumulative production, C)

These polonium isotopes are produced either directly and through decay of the precursor At isobars. The cumulative cross-sections have been obtained as a weighted mean of, respectively, three, three, four and two γ -lines.

Table III

Cross-sections for production of At isotopes. The original cross-sections from Thomas *et al.*² have been multiplied by a factor 3, as discussed in Section 3. The numbers in parenthesis, after each cross section value, give the percentage error.

Energy MeV	201 At			202 At			203 At			204 At			205 At			206 At	
	ref. 2 mb	ref. 1 mb	ref. 2 mb	ref. 1 mb	ref. 2 mb	P.W. ^{*)} mb	ref. 1 mb	ref. 2 mb	P.W. ^{*)} mb	ref. 1 mb	ref. 2 mb	P.W. ^{*)} mb	ref. 1 mb	ref. 2 mb	P.W. ^{*)} mb	ref. 1 mb	P.W. ^{*)} mb
50.3													10.1(17)			24.5(16)	
57.0																	4.8(15)
59.5													109.5(14)			51.5(16)	
60.0														60.7(22)			
62.0															103.9(15)		104.9(15)
63.0													215.3(13)	220.8(23)		40.9(15)	
66.0													233.7(14)				
67.0													294.4(13)	353.4(23)	306.7(15)	34.9(30)	48.7(15)
70.0													349.6(14)	505.2(27)			
70.5									7.5(42)								
72.0										67.2(15)					449.4(15)		17.8(15)
72.5								110.2(20)					294.4(13)			6.9(18)	
73.0									144.0(25)					552.0(25)			
74.6								225.6(15)					215.3(14)				
76.0									255.0(26)								
76.5														208.5(25)			
77.0										280.4(15)					268.1(16)		4.6(15)
77.3								319.3(15)					169.3(15)				
79.0				2.9(16)				291.5(16)	334.5(24)				100.3(15)	93.9(23)			
81.4				27.2(18)				314.1(18)					60.7(18)				
81.5						18.9(24)			196.8(26)					51.9(26)			
82.0										414.9(15)					97.3(15)		
82.7				30.0(18)				306.9(18)					49.7(16)				
84.0				40.1(18)	40.2(23)			315.2(16)	269.4(21)				40.5(18)	44.1(36)			
84.8				78.4(16)				268.8(16)					23.2(16)				
85.0				78.4(16)				279.1(16)					23.9(16)				
86.5					111.6(29)												
86.6				103.3(16)				328.6(16)					15.6(16)				
87.0						48.9(15)									27.6(15)		
88.0				102.4(21)				237.0(35)					16.9(25)				
89.0					270.9(27)												
91.5	14.6(30)			149.6(15)				190.5(16)					15.8(25)				
92.0			1.35(45)		296.4(27)	112.1(15)						188.5(15)					
92.3	16.5(30)			146.9(20)				126.7(24)					4.0(21)				
94.5					190.2(23)				123.5(30)								
96.5					93.6(26)									7.8(43)			
97.0						104.9(16)				79.0(15)							
99.5					112.5(27)												
102.5	1.1(32)		51.0(20)		80.1(24)												
104.0			72.0(21)		66.9(25)												
106.0	7.6(25)		87.0(24)		57.4(26)												
108.0	10.2(20)		135.0(29)		36.0(26)			25.6(40)									
113.0	29.6(23)		69.0(22)		16.7(26)												
114.5	33.8(24)		60.0(17)		20.0(30)												
117.0	35.1(24)				11.1(30)												
118.0			36.0(25)														
119.0	40.2(23)				8.0(41)												

*) Present Work

1 - R.BIMBOT, M.LEFORT, and A.SIMON. J.Phys., 29 (1968) 563.

2 - T.D.THOMAS, G.E.GORDON, R.M.LATIMER and G.T.SEABORG. Phys.Rev. 126 (1962) 1805

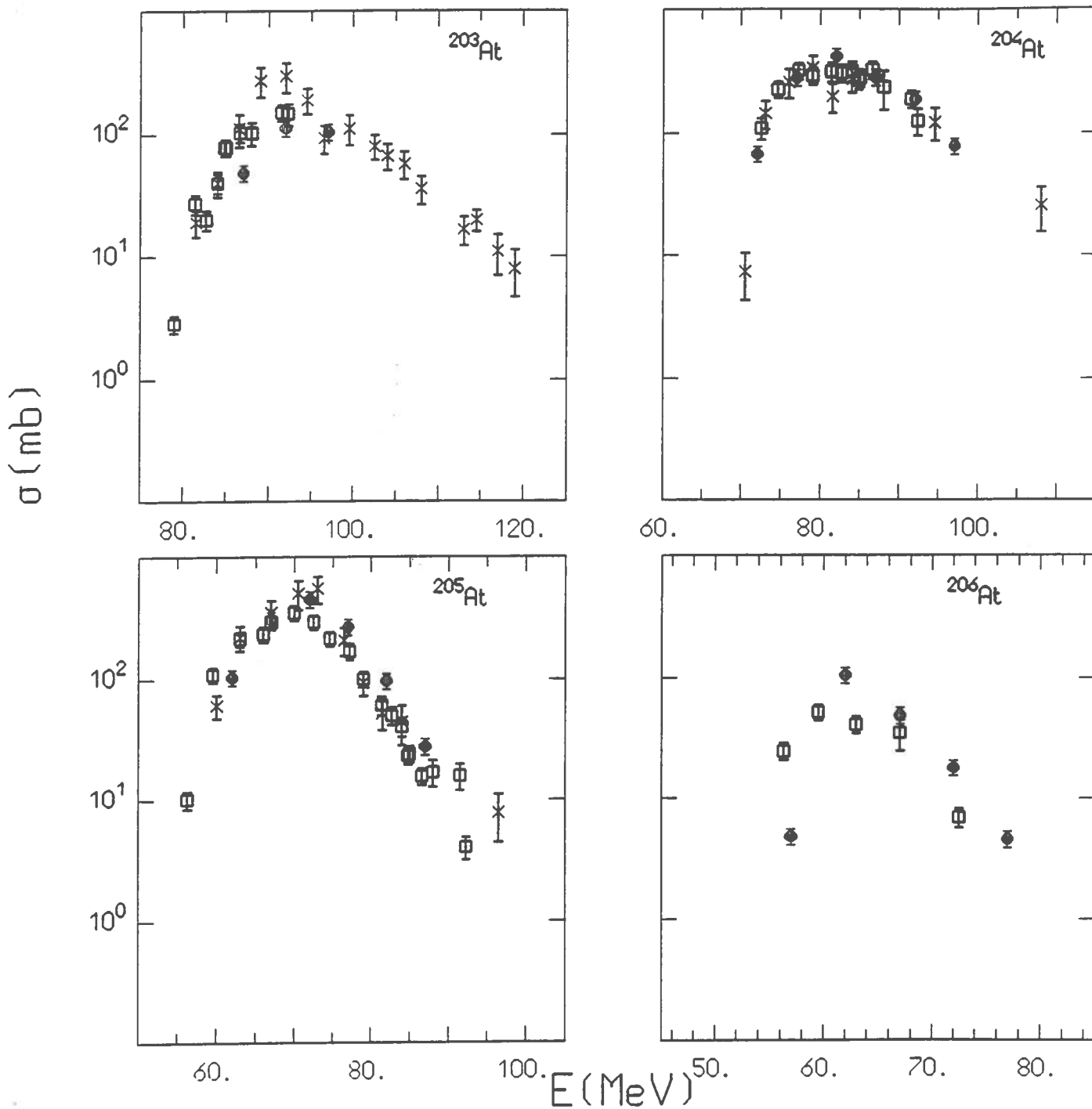


Fig. 1.- Excitation functions for production of ^{203}At , ^{204}At , ^{205}At , and ^{206}At . The experimental data are from present work (solid dots), Bimbot *et al.*⁴ (open squares), Thomas *et al.*³ (crosses). The Thomas *et al.* data have been multiplied by a factor 3, as discussed in Section 3.

The measured cross-sections for production of these isotopes are given in Table IV and shown in Fig. 2 (where the values we measured at 120 MeV in a previous experiment ¹ are also given).

^{203}Bi , ^{202}Bi , $^{201}\text{Bi}^g$, $^{200}\text{Bi}^g$ and $^{199}\text{Bi}^g$ (C)

These Bi isotopes may be produced either through decay of the precursors At and Po isobars produced in a complete fusion (CF) reaction or, independently, by two processes: CF followed by emission of an α -particle and 2 to 6 neutrons (a rather small contribution) or, as already suggested by Bimbot *et al.*,⁵ in the incomplete fusion (ICF) of a ^8Be followed by neutron emission. As a consequence, the excitation functions for production of these isotopes appear more structured than the excitation functions for production of At and Po isotopes.

In the case of ^{203}Bi and ^{202}Bi the threshold for the ICF contribution (evaluated considering the energy needed by ^{12}C to breaking-up into an α -particle and a ^8Be , the Coulomb energy of the α emitted in the break-up and the binding energy of the ^8Be and the neutrons in ^{205}Bi created in the ICF) is of the order of the observed threshold. In the case of the other three isotopes ^{201}Bi , ^{200}Bi , and ^{199}Bi the threshold for the ICF contribution is, respectively, ≈ 75 , 85 and 100 MeV.

The threshold for the CF processes coincides in all the cases with the observed threshold of the excitation functions.

The cross-sections for production of all the isotopes have been obtained as a weighted mean of the values obtained by the analysis of at least two γ -lines.

The measured cross-sections for production of Bi isotopes are given in Table V and shown by solid dots in Fig. 3 where, as in the case of Po isotopes, also the values we measured at 120 MeV¹ are given.

$^{201}\text{Pb}^g$, ^{200}Pb , and $^{199}\text{Pb}^g$ (C)

These Pb isotopes may be produced either through decay of the precursors At, Po, and Bi isobars produced in a CF process or of the Bi isobars produced in a ICF reaction or, independently, through ICF of a ^8Be followed by emission of one proton

Table IV
Cross-sections for production of Po isotopes

^{202}Po		$^{203}\text{Po}^g$	^{204}Po	^{205}Po
Energy MeV	P.W.*) mb	P.W.*) mb	P.W.*) mb	P.W.*) mb
62.0				136.2(15)
67.0				438.8(15)
72.0			87.6(15)	577.8(15)
77.0			367.6(15)	369.6(15)
82.0		23.4(15)	511.7(15)	132.7(15)
87.0		121.9(15)	360.9(15)	34.1(15)
92.0	6.2(15)	291.1(15)	269.9(15)	17.9(15)
97.0	57.1(15)	323.6(15)	115.1(15)	5.5(15)
120.0 ¹⁾	140.0(06)	30.0(03)	6.7(10)	

*) Present Work

1 - D.J.PARKER, P.VERGANI, E.GADIOLI, J.J.HOGAN,
F.VETTORE, E.GADIOLI-ERBA, E.FABRICI and
M.GALMARINI, Phys. Rev. C44, 1528 (1991)

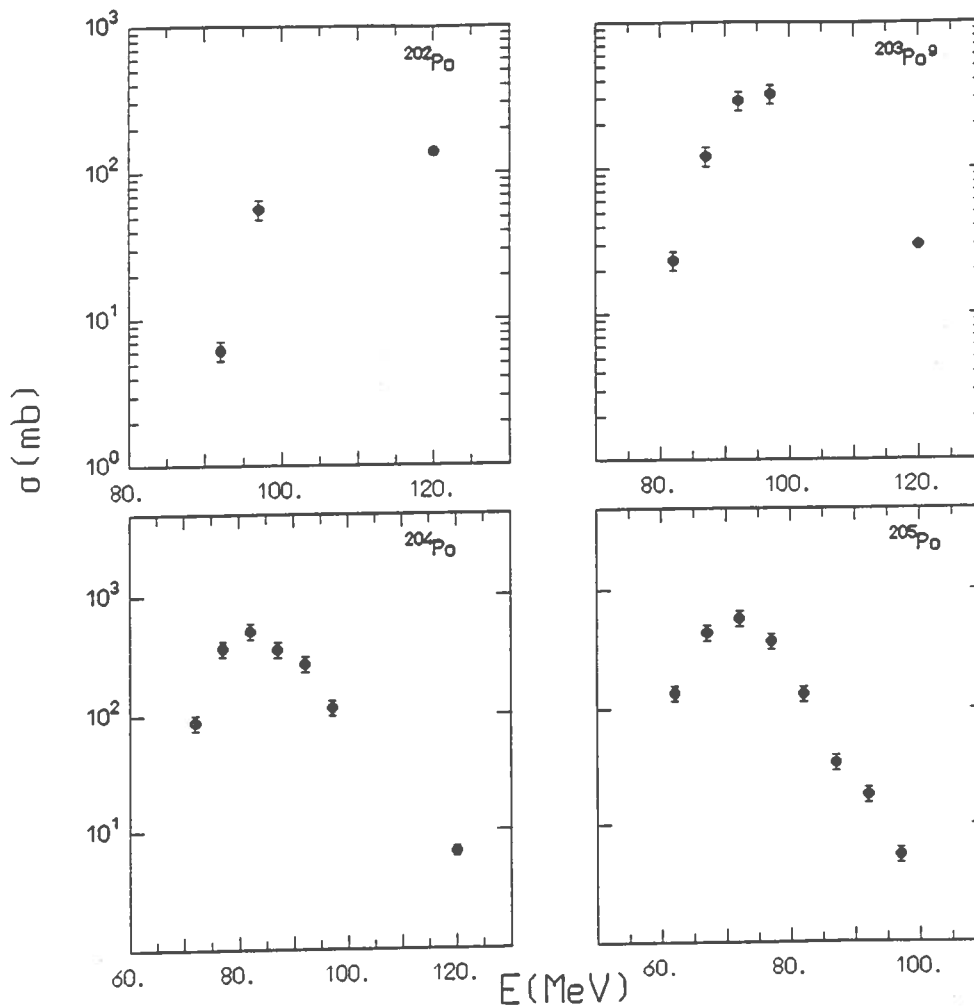


Fig. 2.- Excitation functions for production of ^{202}Po , $^{203}\text{Po}^g$, ^{204}Po , and ^{205}Po . Up to 97 MeV, the cross-sections are from present work. The value at 120 MeV is from Ref. [1].

Table V
Cross-sections for production of Bi isotopes

Energy MeV	$^{199}\text{Bi}^g$		$^{200}\text{Bi}^g$		$^{201}\text{Bi}^g$		^{202}Bi		^{203}Bi		^{204}Bi
	P.W.*) mb	P.W.*) mb	Ref. 1 mb	P.W.*) mb	Ref. 1 mb	P.W.*) mb	Ref. 1 mb	P.W.*) mb	Ref. 1 mb	P.W.*) mb	Ref. 1 mb
62.0				12.3(15)		4.5(15)					
66.0			18.0(26)		12.5(18)			12.7(19)			
67.0				40.0(15)		19.0(15)					
68.8			34.5(17)		26.3(19)			15.3(15)			
71.6			41.0(23)		42.2(18)			13.6(16)			46.2(16)
72.0		3.1(15)		61.9(15)		39.7(15)					
74.4			43.6(21)					9.73(14)			145.6(16)
77.0		13.7(15)	36.2(24)	43.9(15)	73.3(16)	56.7(15)		7.2(15)			283.3(16)
80.0			37.1(29)		89.9(22)			10.4(10)			416.7(16)
82.0		19.9(15)		45.3(15)		54.7(15)			20.3(15)		
82.7			47.1(19)		85.6(17)			29.0(14)			458.9(15)
85.3			60.6(17)		104.1(19)			73.9(15)			426.7(15)
87.0		15.7(15)		59.5(15)		38.5(15)	150.9(11)	121.9(15)			
87.8	21.0(15)		78.1(15)		68.2(19)						355.6(16)
92.0	48.3(15)	25.0(15)		128.9(15)		48.4(15)			397.2(15)		
97.0	45.1(15)	48.2(15)		132.2(15)		111.0(15)			403.4(15)		
120.0 ²⁾	120.0(13)	111.0(06)		100.0(30)		280.0(05)			41.0(12)		

*) Present Work

- 1 - R.BIMBOT, D. GARDES, and M.F.RIVET, Nucl. Phys. A189 (1972) 193
- 2 - D.J.PARKER, P.VERGANI, E. GADIOLI, J.J.HOGAN, F.VETTORE, E.GADIOLI-ERBA, E.FABRICI and M.GALMARINI, Phys. Rev. C44, 1528 (1991)

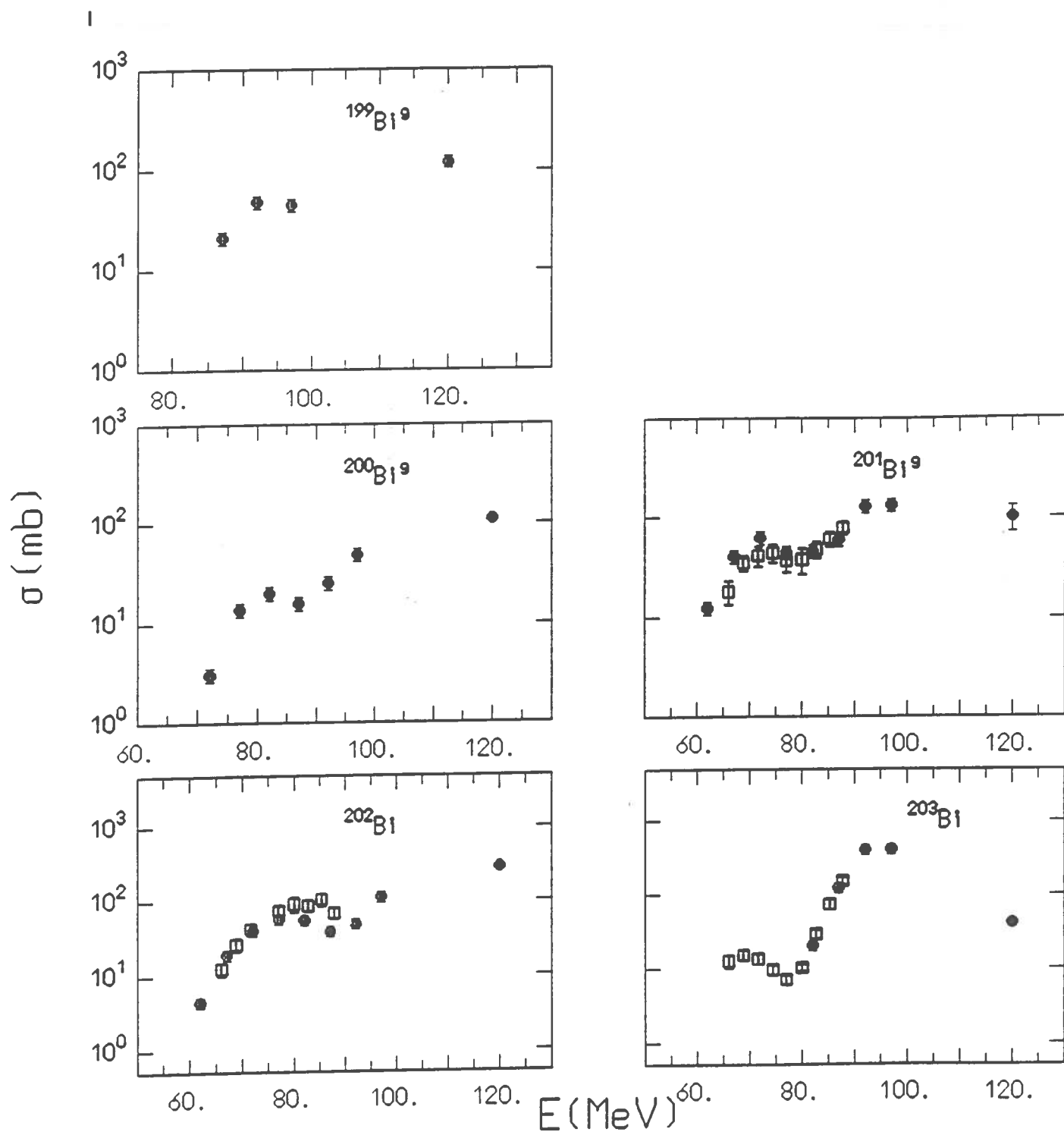


Fig. 3.- Excitation functions for production of $^{199}\text{Bi}^g$, $^{200}\text{Bi}^g$, $^{201}\text{Bi}^g$, ^{202}Bi , and ^{203}Bi . The solid dots give the experimental cross-sections from present work (up to 97 MeV) and from Parker *et al.*¹ (at 120 MeV); the open squares give the values of Bimbot *et al.*⁵.

and 3 to 5 neutrons. The possibility of independent production through CF followed by emission of an α -particle and a proton and the needed number of neutrons is too unlikely to contribute significantly. The threshold for ICF processes in the three cases is equal to, respectively, $\approx 75, 85$ and 100 MeV, while the threshold for the CF processes coincides with the observed threshold of the excitation functions.

The cross sections for production of the three isotopes have been obtained as a weighted mean of the values obtained by the analysis of two γ -lines.

The measured cross-sections for production of Pb isotopes are given in Table VI and shown by solid dots in Fig. 4 where also the value we measured at 120 MeV^1 are given.

$^{198}\text{Tl}^m$ (I)

The dominant contribution to the independent production of this residue is the ICF of one α -particle followed by emission of three neutrons. The cross-sections are obtained as a weighted mean of the values obtained by the analysis of two γ -lines.

^{199}Tl , and $^{198}\text{Tl}^g$ (C)

These two residues may be produced (at energies exceeding, respectively, ≈ 78 and 90 MeV) through decay of the precursor isobars produced in CF. At energies exceeding, respectively, ≈ 75 and 85 MeV they are produced both independently and through decay of precursor isobars produced in the ICF of a ^8Be . At lower energies they may be produced only independently through ICF of one α -particle followed by emission of two or three neutrons.

The measured cross-sections for production of Tl isotopes are given in Table VII and shown by solid dots in Fig. 5 where also the values we measured at 120 MeV^1 are given.

3. Comparison with previous experimental information.

The excitation functions for production of At isotopes, in ranges of incident

Table VI
Cross-sections for production of Pb isotopes

Energy MeV	$^{199}\text{Pb}^g$	^{200}Pb	$^{201}\text{Pb}^g$
	P.W.*) mb	P.W.*) mb	P.W.*) mb
62.0			12.0(15)
67.0			42.5(15)
72.0			64.5(15)
77.0		24.7(15)	47.5(15)
82.0	12.7(15)	34.0(15)	44.9(15)
87.0	38.1(15)	27.9(15)	110.1(15)
92.0	101.6(15)	49.1(15)	157.3(15)
97.0	117.3(15)	92.0(15)	169.9(15)
120.0 ¹⁾	150.0(13)	160.0(12)	150.0(03)

*) Present Work

- 1 - D.J.PARKER, P.VERGANI, E.GADIOLI, J.J.HOGAN,
F.VETTORE, E.GADIOLI-ERBA, E.FABRICI and
M.GALMARINI, Phys. Rev. C44, 1528 (1991)

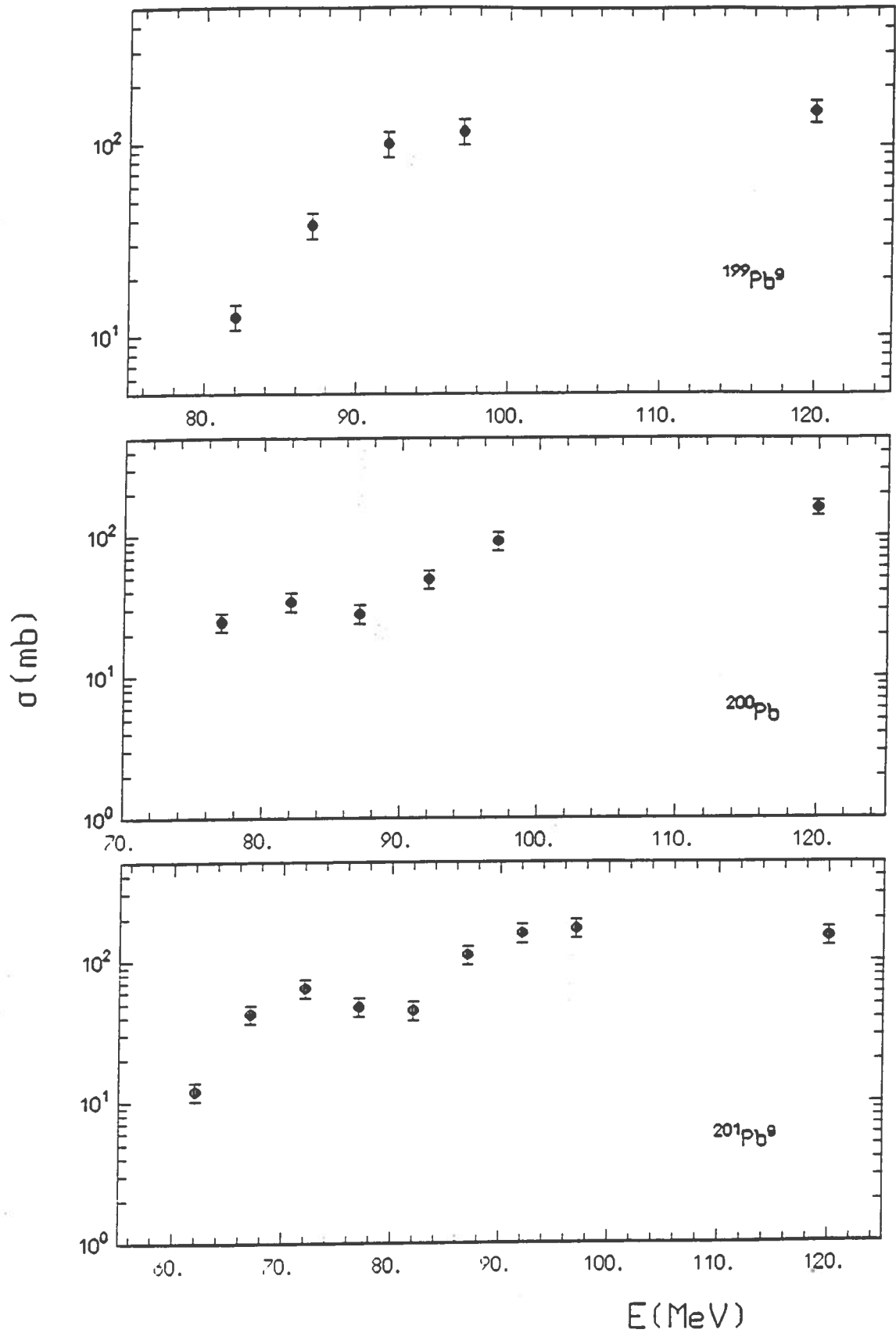


Fig. 4.- Excitation functions for production of ^{199}Pb , ^{200}Pb , and ^{201}Pb . Up to 97 MeV, the cross-sections are from present work. The value at 120 MeV is from Ref. [1].

Table VII
Cross-sections for production of Tl isotopes

Energy MeV	$^{198}\text{Tl}^g$	$^{198}\text{Tl}^m$	^{199}Tl	
	P.W. *) mb	P.W. *) mb	Ref. 1 mb	P.W. *) mb
62.0				4.5(15)
67.0				9.5(15)
72.0	3.8(15)			26.4(15)
77.0	8.3(15)	6.8(15)	21.6(26)	35.2(15)
80.0			40.4(20)	
82.0	13.9(15)	10.0(15)		57.4(15)
82.7			54.6(18)	
85.3			59.2(21)	
87.0	16.4(15)	14.4(15)		86.3(15)
87.8			59.2(27)	
92.0	36.3(15)	31.5(15)		192.3(15)
97.0	71.4(15)	44.9(15)		212.0(15)
120.0 ²⁾	134.1(06)	66.0(05)		199.0(05)

*) Present Work

- 1 - R.BIMBOT, D. GARDES, and M.F.RIVET,
Nucl. Phys. A189 (1972) 193
- 2 - D.J.PARKER, P.VERGANI, E.GADIOLI,
J.J.HOGAN, F.VETTORE, E.GADIOLI-ERBA,
E.FABRICI and M.GALMARINI,
Phys. Rev. C44, 1528 (1991)

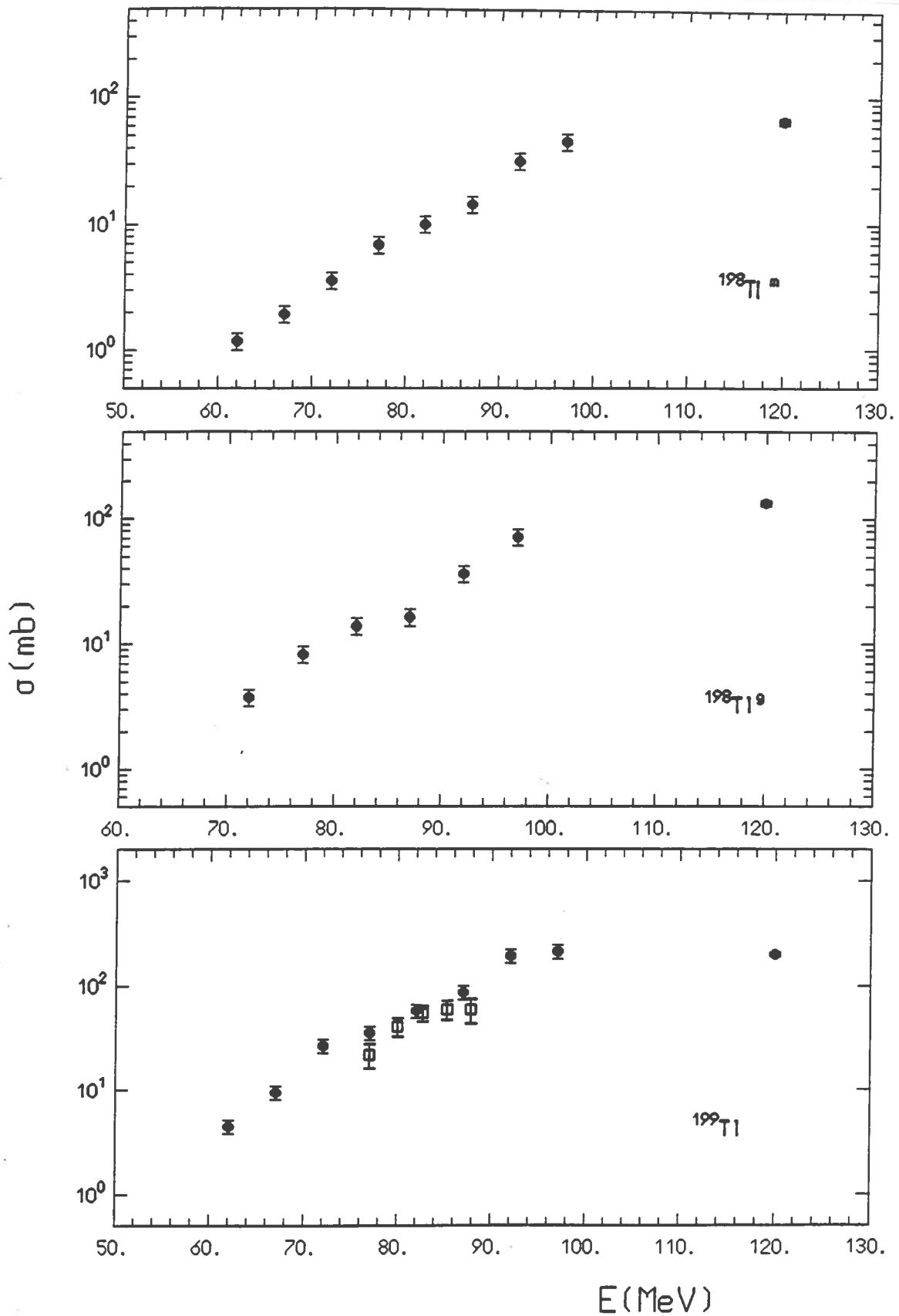


Fig. 5.- Excitation functions for production of $^{198}\text{Tl}^m$, $^{198}\text{Tl}^g$, and ^{199}Tl . The solid dots give the experimental cross-sections from present work (up to 97 MeV) and from Parker *et al.*¹ (at 120 MeV); the open squares give the values of Bimbot *et al.*⁵.

^{12}C energies overlapping with that of present measurement, have been measured by Thomas *et al.*³ ($^{205-203}\text{At}$, between 60 and 120 MeV), Bimbot *et al.*⁴ ($^{206-203}\text{At}$, between ≈ 56 and 92 MeV), and Stickler and Hofstetter⁶ ($^{206-203}\text{At}$, between 66 and ≈ 125 MeV).

The first two experiments, considerably more involved than ours, measured the α activity of the At isotopes with an ionization chamber and (Bimbot *et al.*⁴, in the case of ^{204}At and ^{203}At) a semiconductor Si counter and involved the chemical separation of all (Thomas *et al.*³) or part (Bimbot *et al.*⁴) of the At isotopes. In the third experiment, the induced γ -ray activity was measured with Ge(Li) detectors. Many of the cross-sections reported by these authors had to be corrected since the abundances they used for the characteristic α or γ lines differ from the values presently adopted.¹⁰

The excitation function for production of the At isotopes, both measured in this work and given by previous authors are shown in Fig. 6.

Our results are in agreement with those of Bimbot *et al.*⁴. The cross-sections given by Thomas *et al.*³ are always considerably smaller in absolute value than those measured in this experiment and by Bimbot *et al.*⁴; however their energy dependence is nearly the same as that found in these works suggesting that these data could be simply re-normalised to the present and to the Bimbot *et al.*⁴ data.

In Fig. 7 the experimental cross-sections for production of $^{203,204,205}\text{At}$ given by Thomas *et al.*³ multiplied by a factor 3 are compared to the average of the cross-sections measured in this work and in the experiment by Bimbot *et al.*⁴ (the averaged cross-sections are given by the full lines, those of Thomas *et al.*³ by the crosses with error bars). The experimental procedure of Thomas *et al.*³ is quite complex and to assume that their excitation functions, which extend over an energy range of great interest for the subsequent theoretical analysis, should be re-normalised to bring them in agreement with the more recent experimental results is not unreasonable.

The data of Stickler and Hofstetter⁶ display a capricious trend. Sometimes they are consistent with our data and those of Bimbot *et al.*⁴ (in the case of ^{206}At and ^{205}At at energies exceeding 75 MeV) sometimes they completely disagree displaying unreasonable high thresholds (in the case of ^{204}At and ^{203}At). We have not found

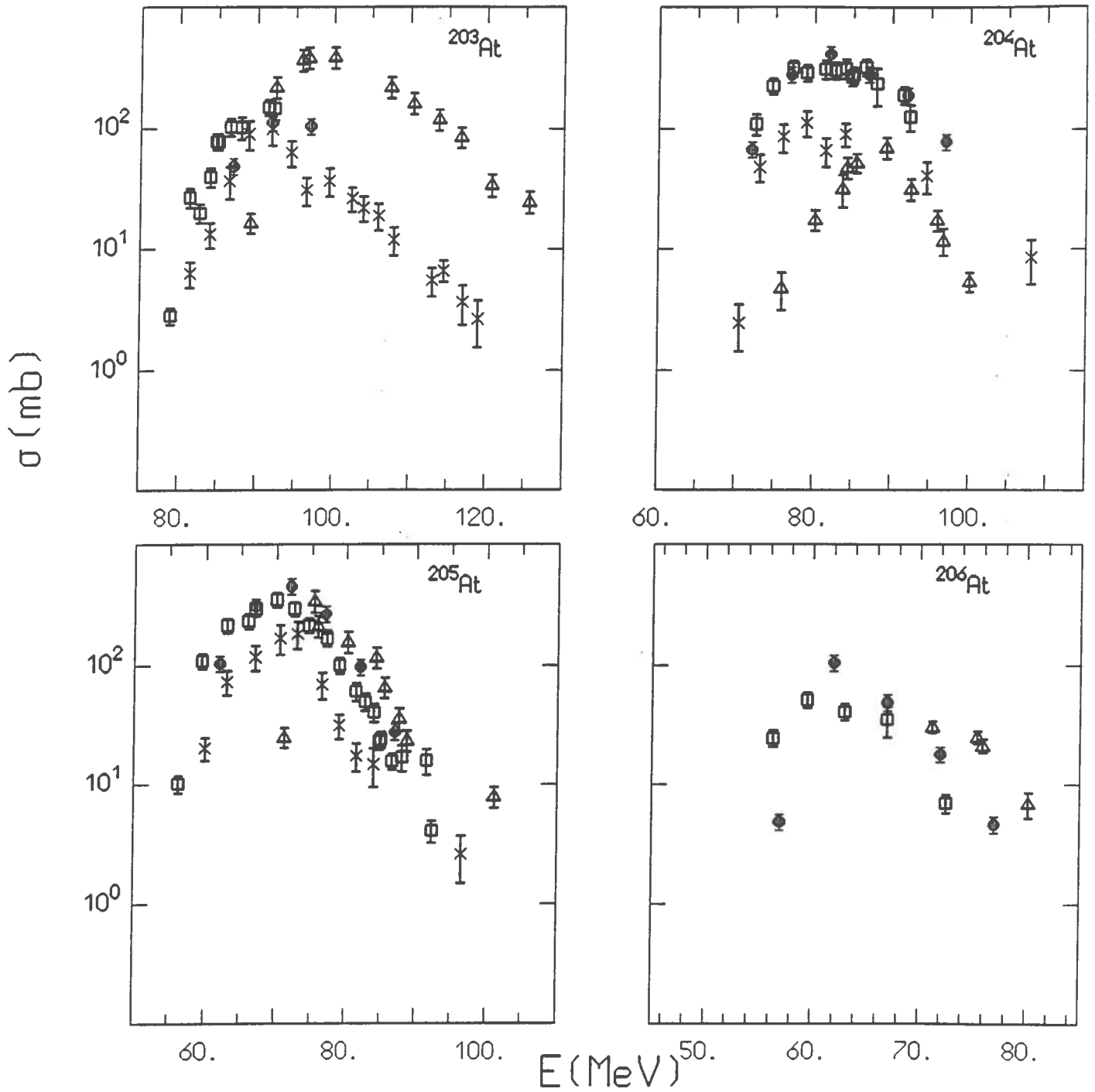


Fig. 6.- Excitation functions for production of ^{203}At , ^{204}At , ^{205}At , and ^{206}At . The experimental data are from present work (solid dots), Bimbot *et al.*⁴ (open squares), Thomas *et al.*³ (crosses), and Stickler and Hofstetter⁶ (open triangles).

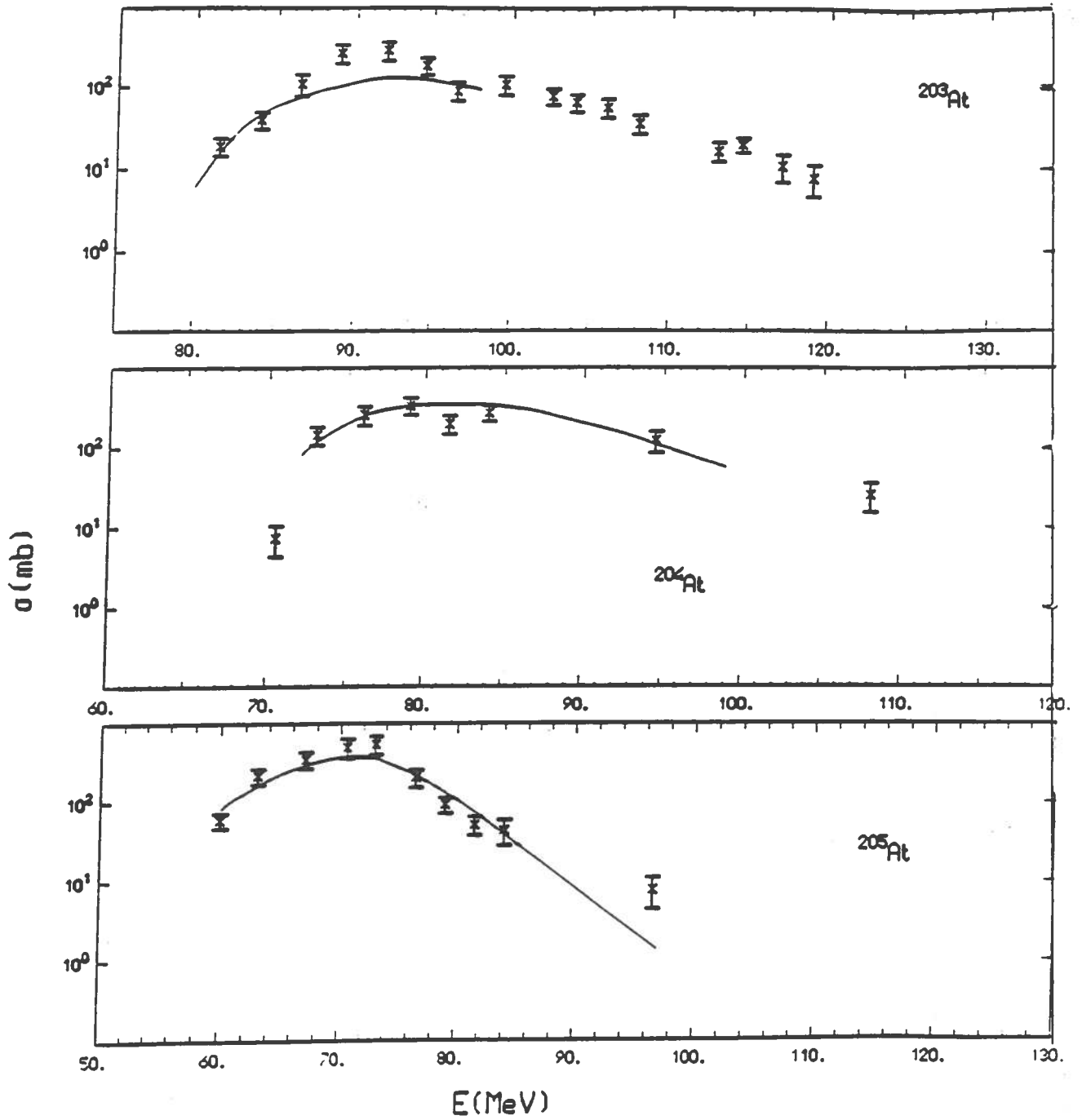


Fig. 7.- The full lines give the cross-sections for production of ^{203}At , ^{204}At , and ^{205}At obtained as an average of the values measured in present work and by Bimbot *et al.*⁴. The crosses the values given by Thomas *et al.*³ multiplied by a factor 3.

any simple explanation to justify their disagreement with ours and Bimbot *et al.*⁴ data.

Our data, the Bimbot *et al.*⁴ data, and the re-normalised Thomas *et al.*³ data are shown in Fig. 1. The Bimbot *et al.*⁴ data and the re-normalised Thomas *et al.*³ data are also reported together with ours in Table III.

The excitation functions for production of ^{203,202,201g}Bi and ¹⁹⁹Tl have been measured by Bimbot *et al.*⁵ between ≈ 62 and 88 MeV through detection of the induced γ activity. These authors also measured the heavy residue angular distributions. This allowed them to separate ICF from CF processes, since an ICF process originates residues with an angular distribution peaked to an angle substantially greater than 0° ($\approx 17^\circ$ for the ICF of a ⁸Be at the energies they consider). Thus they found sizeable cross-section for ICF of a ⁸Be or an α particle even at incident energies only slightly higher than Coulomb barrier.

The cross-sections measured by these authors (some of them had to be slightly corrected using more recent values for the abundances of CGL) are in good agreement with ours as shown in Figs. 3 and 5.

4. Reaction cross-sections.

In Fig. 8 are shown, in the energy range from ≈ 56 to ≈ 100 MeV, the excitation functions for independent production of the At isotopes with mass 206 to 202, and the Po isotopes with mass 205 to 203. The cross-sections for production of the At isotopes are an average of the values measured in this and in the Bimbot *et al.*⁴ experiment (except in the case of ²⁰²At where they are an average between the Bimbot *et al.*⁴ and the Thomas *et al.*³ data multiplied by a factor 3). Those for production of the Po isotopes are evaluated by subtracting from the cumulative cross-sections those due to the decay of the precursor At isobars both measured in this work.

Even considering that only some of the experimental errors affecting the cumulative cross-sections for production of Po and the independent cross-section for production of At add statistically in deriving the uncertainty of the independent

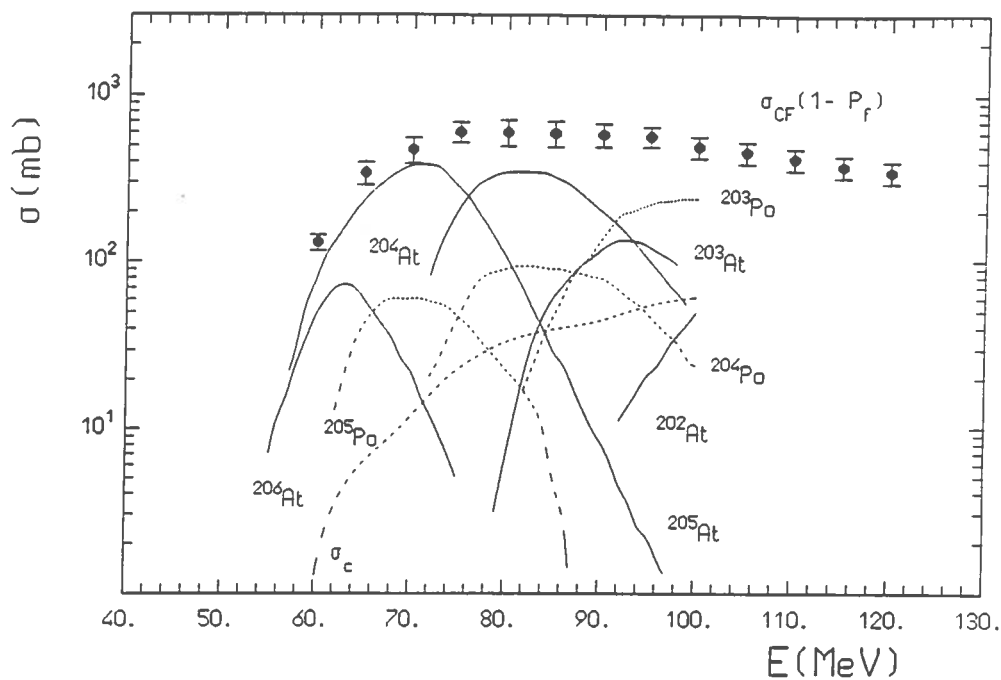


Fig. 8.- Cross-sections for production, in a CF reaction, of $^{206,205,204,203,202}\text{At}$, $^{205,204,203}\text{Po}$, the isotopes of Bi and lower Z nuclei (σ_c), and cross section for complete fusion and subsequent decay by particle emission, $\sigma_{CF}(1 - P_F)$.

Table VIII
Cross-sections contributing to the reaction cross-section of ^{13}C with ^{197}Au between 60 and 120 MeV

E(MeV)	$\sigma_{CF}(1 - P_F)$	σ_F	σ_{Be}	σ_α	σ_R	σ_{Thomas}
60	130 ± 14				130 ± 14	145
65	343 ± 55	65 ± 7	16 ± 2	16 ± 2	440 ± 56	364
70	474 ± 83	120 ± 12	44 ± 7	29 ± 4	667 ± 84	597
75	606 ± 85	220 ± 22	80 ± 12	50 ± 8	956 ± 89	814
80	604 ± 109	340 ± 34	118 ± 18	74 ± 11	1136 ± 116	1024
85	594 ± 105	490 ± 49	139 ± 21	85 ± 13	1308 ± 118	1205
90	584 ± 92	600 ± 60	148 ± 22	96 ± 14	1428 ± 113	1368
95	570 ± 81	730 ± 73	163 ± 24	105 ± 16	1568 ± 113	1521
100	495 ± 73	830 ± 83	180 ± 27	113 ± 17	1618 ± 115	1660
105	460 ± 69	950 ± 95	195 ± 29	121 ± 18	1726 ± 122	1817
110	420 ± 63	1000 ± 100	213 ± 32	130 ± 20	1763 ± 124	1896
115	380 ± 57	1100 ± 110	235 ± 35	140 ± 21	1855 ± 130	2000
120	350 ± 53	1170 ± 117	260 ± 39	150 ± 23	1930 ± 136	2099

cross-sections for production of Po, these last cross-sections are affected by a large statistical error that in some cases exceeds 50%.

In Fig. 8, $\sigma_{CF}(1 - P_F)$, the total reaction cross-section for formation of the composite nucleus ^{209}At in a CF reaction and its subsequent decay by emission of several particles without fission is also shown. Up to about 100 MeV, this cross-section is given by the sum of the cross-sections for production of the At and the Po isotopes, that for emission of α particles in addition to neutrons and that, almost negligible, for emission of two charged particles in addition to neutrons.

The two last contributions are not measured values but values estimated by a theoretical calculation¹⁴. In the energy interval considered, they never exceed $\approx 10\%$ of the cross-section for production of At and Po isotopes.

In the interval 100 to 120 MeV, the values of $\sigma_{CF}(1 - P_F)$ are interpolated between the previous values and the value obtained from the analysis of the recoil range distributions at 120 MeV¹. The values of $\sigma_{CF}(1 - P_F)$ are also reported in Table VIII.

This Table also gives the values of the reaction cross-section σ_R obtained as a sum of $\sigma_{CF}(1 - P_F)$, the fission cross-section σ_F , and σ_{Be} and σ_α , the cross-sections for, respectively, ICF of a ^8Be and an α -particle. σ_F has been measured by Gordon *et al.*¹⁵. For incident energies below 90 MeV, σ_{Be} are those measured by Bimbot *et al.*⁵ diminished by the estimated contribution of α 's evaporated from the composite nucleus ^{209}At created in a CF¹⁴. At 120 MeV we took for this cross-sections the values found by Parker *et al.*¹, and between 90 and 120 MeV values interpolated linearly on a logarithmic scale. The cross-sections σ_α are those given by Bimbot *et al.*⁵ below 80 MeV, by Parker *et al.*¹ at 120 MeV and an almost linear interpolation on a logarithmic scale at intermediate energies.

In Fig. 9. the product of the incident channel energy of C ions times the reaction cross-section, $E_{ch} \cdot \sigma_R$, is reported as a function of E_{ch} to obtain the interaction barrier V_{int} and the interaction radius R_{int} through the relation¹⁶

$$E_{ch} \cdot \sigma_R = \pi R_{int}^2 (E_{ch} - V_{int}).$$

The values thus obtained are $V_{int}=57.3$ MeV, and $R_{int}=10.75$ fm.

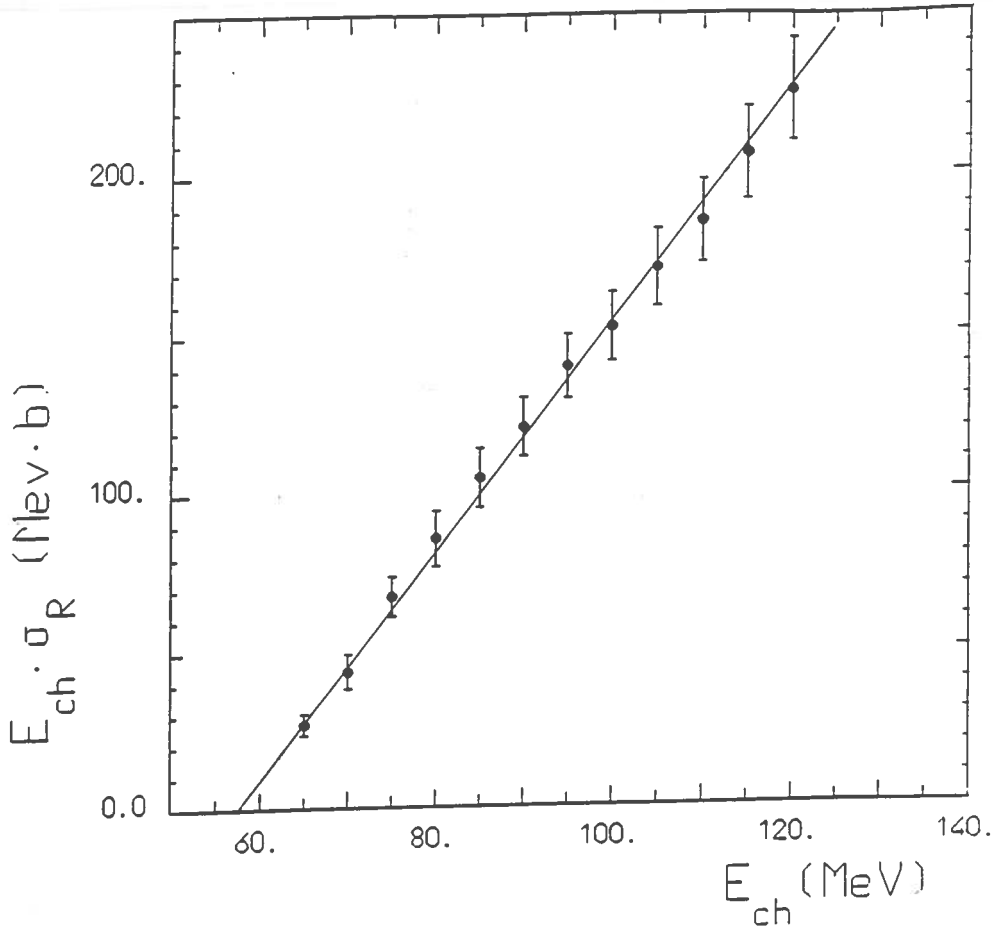


Fig. 9.- Plot of $E_{ch} \cdot \sigma_R$ vs. E_{ch} to obtain the interaction barrier V_{int} and the interaction radius R_{int} .

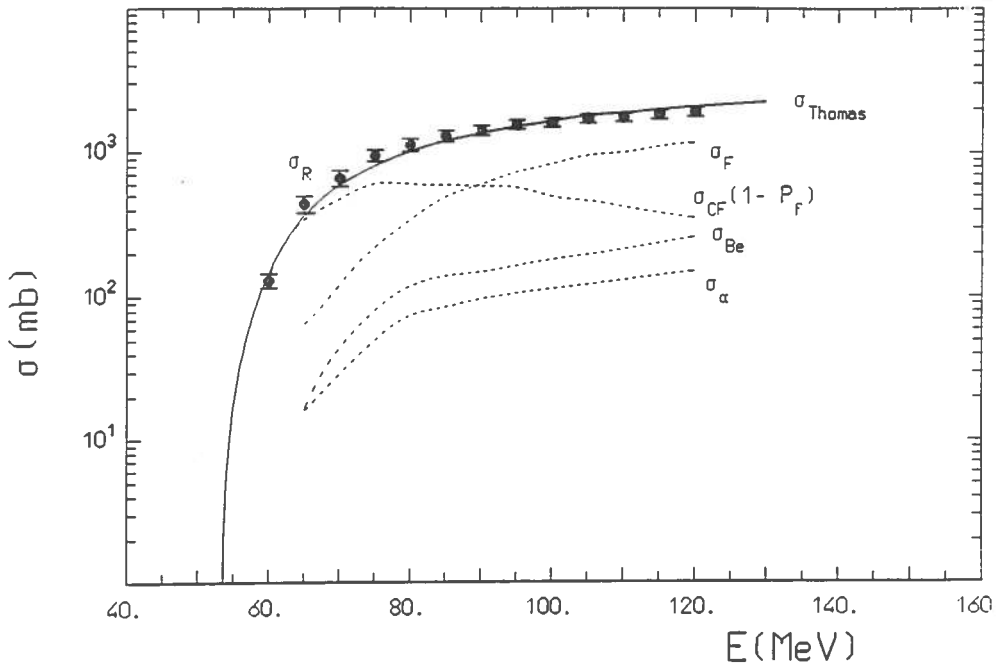


Fig. 10.- Cross-sections for: complete fusion and subsequent decay by particle emission ($\sigma_{CF}(1 - P_F)$), fission (σ_F), ICF of a ${}^8\text{Be}$ fragment (σ_{Be}), and an α particle (σ_α). The solid dots give the total reaction cross-section (σ_R), which is compared with that evaluated by Thomas¹⁷.

The reaction cross-section σ_R is in excellent agreement with that, frequently used in literature, estimated by Thomas¹⁷.

Acknowledgements

Thanks are due to S. Filice, G. P. Fattori and F. Tomasi for their generous help in the course of this work.

Appendix

If a precursor, p , is produced during the irradiation with cross-section σ_p and decays with a decay constant λ_p and a branching ratio P_p to a daughter nucleus d which during the irradiation is produced with cross-section σ_d and decays with decay constant λ_d , the following equations hold for $t \leq T$, where T is the irradiation time:

$$\frac{dN_p}{dt} = \sigma_p \tau \phi(t) - \lambda_p N_p \quad [A.1]$$

$$\frac{dN_d}{dt} = \sigma_d \tau \phi(t) + P_p \lambda_p N_p - \lambda_d N_d, \quad [A.2]$$

where τ is the number of target nuclei per cm² and $\phi(t)$ is the flux of incident ions in particles per second, while for $t \geq T$:

$$\frac{dN_p}{dt} = -\lambda_p N_p \quad [A.3]$$

$$\frac{dN_d}{dt} = -\lambda_d N_d + P_p \lambda_p N_p. \quad [A.4]$$

To solve these coupled decay equations, one multiplies [A.1] and [A.3] by $\frac{P_p \lambda_p}{\lambda_p - \lambda_d}$ and one adds these equations to, respectively, [A.2] and [A.4].

One thus obtains for $t \leq T$:

$$\frac{d}{dt} \left(N_d + \frac{P_p \lambda_p}{\lambda_p - \lambda_d} N_p \right) = \left(\sigma_d + \frac{P_p \lambda_p}{\lambda_p - \lambda_d} \sigma_p \right) \tau \phi(t) - \lambda_d \left(N_d + \frac{P_p \lambda_p}{\lambda_p - \lambda_d} N_p \right), \quad [A.5]$$

and for $t \geq T$

$$\frac{d}{dt} \left(N_d + \frac{P_p \lambda_p}{\lambda_p - \lambda_d} N_p \right) = -\lambda_d \left(N_d + \frac{P_p \lambda_p}{\lambda_p - \lambda_d} N_p \right). \quad [A.6]$$

Equation [A.5] shows that the quantity $C(t) = N_d + \frac{P_p \lambda_p}{\lambda_p - \lambda_d} N_p$ varies during the irradiation time as if it is produced with cross-section $\sigma_c = \sigma_d + \frac{P_p \lambda_p}{\lambda_p - \lambda_d} \sigma_p$.

At the end of irradiation one thus obtains

$$C_0 \equiv C(T) = \left(\sigma_d + \frac{P_p \lambda_p}{\lambda_p - \lambda_d} \sigma_p \right) \tau \Phi_{\lambda_d}, \quad [A.7]$$

where

$$\Phi_{\lambda_d} = e^{-\lambda_d T} \int_0^T \phi(t) e^{\lambda_d t} dt. \quad [A.8]$$

Equation [A.6] shows that at times greater than T

$$N_d + \frac{P_p \lambda_p}{\lambda_p - \lambda_d} N_p = C_0 e^{-\lambda_d t}. \quad [A.9]$$

Since

$$N_p = N_p(T) e^{-\lambda_p t}, \quad [A.10]$$

the number of daughter nuclei varies with time with the law:

$$N_d = C_0 e^{-\lambda_d t} - \frac{P_p \lambda_p}{\lambda_p - \lambda_d} N_p(T) e^{-\lambda_p t}. \quad [A.11]$$

If $\lambda_p \gg \lambda_d$, for $t \rightarrow \infty$ the second term becomes negligible in comparison with the first and

$$N_d \rightarrow C_0 e^{-\lambda_d t} \quad [A.12]$$

Thus if one reproduces this part of the decay curve by a simple exponential, one obtains the activity of daughter d at the end of the irradiation as $C(T) \cdot \lambda_d$ and the cumulative cross section as

$$\sigma_c = \sigma_d + \frac{P_p \lambda_p}{\lambda_p - \lambda_d} \sigma_p. \quad [A.13]$$

The procedure is easily generalised to the case of several precursors. Thus in the case of the sequence



with decay constants

$$\lambda_A \gg \lambda_B \gg \lambda_C, \quad [A.14]$$

and branching ratios P_A and P_B , one obtains the cumulative cross-section for production of C given by

$$\sigma_c^C = \sigma_i^C + \frac{\lambda_B}{\lambda_B - \lambda_C} \sigma_i^B P_B + \frac{\lambda_A \lambda_B}{(\lambda_A - \lambda_C)(\lambda_B - \lambda_C)} \sigma_i^A P_A P_B. \quad [A.15]$$

The procedure shown does not hold (either in the case of single precursor and in the case of several precursors) if the decay constants do not satisfy [A.14], since in this case all terms contributing to $N_d(t)$ have to be considered whatever time interval is taken.

References

- 1 - D.J.Parker, P.Vergani, E.Gadioli, J.J.Hogan, F.Vettore, E.Gadioli Erba, E.Fabrizi and M.Galmarini, *Phys. Rev.* **C44**, 1528 (1991)
- 2 - E. Gadioli, P. Vergani, F. Vettore, D.J.Parker, J.J.Hogan, E.gadioli Erba, E.Fabrizi, M.Galmarini and E.Vaciago, *Proceedings of the 6th International Conference on Nuclear Reaction Mechanisms*, Varenna, 1991, Edt. E.Gadioli, *Ricerca Scientifica ed Educazione Permanente*, Suppl. N. 84, pg. 76
- 3 - T. D. Thomas, G. E. Gordon, R. M. Latimer and G. T. Seaborg, *Phys. Rev.* **126**, 1805 (1962)
- 4 - R. Bimbot, M. Lefort and A. Simon, *J. Phys. (Paris)* **29**, 563 (1968)
- 5 - R. Bimbot, D. Gardes and M. F. Rivet, *Nucl. Phys.* **A189**, 193 (1972)
- 6 - J. D. Stickler and K. J. Hofstetter, *Phys. Rev.* **C9**, 1064 (1974)
- 7 - E. Gadioli *et al.*, to be published
- 8 - J. A. B. Goodall, UKAEA Report AERE-M3185 (1982)
- 9 - J. J. Hogan and D. J. Parker, *private communication*
- 10 - U. Reus, W. Westmeier and I. Warnecke, *At. Data Nucl. Data Tables* **29**, 1 (1983)
- 11 - T. Mopek, T. Vroaa, V. Vasmosv, H. Apostz, V. Noibert and S. Hoinamki, JINR Report No. JINR-P6-4868, 1970 (unpublished)
- 12 - K. K. Seth, *Nucl. Data* **B7**, 161 (1972)
- 13 - P. K. Hopka, R. A. Naumann and E. H. Spejewski, *Nucl. Phys.* **A419**, 63 (1970)
- 14 - P. Vergani *et al.*, to be published
- 15 - G. E. Gordon, A. E. Larsh, T. Sikkeland and G. T. Seaborg, *Phys. Rev.* **C120**, 1341 (1960)
- 16 - R. Bass, *Nuclear Reactions with Heavy Ions*, Springer-Verlag, Berlin, Heidelberg, New York, 1980, pg. 111,
- 17 - T. D. Thomas, *Phys. Rev.* **C116**, 703 (1959)